



Published in final edited form as:

*Biomaterials*. 2016 January ; 77: 66–76. doi:10.1016/j.biomaterials.2015.11.001.

## Super natural killer cells that target metastases in the tumor draining lymph nodes

Siddarth Chandrasekaran<sup>1</sup>, Maxine F. Chan<sup>1</sup>, Jiahe Li<sup>1</sup>, and Michael R. King<sup>1,\*</sup>

<sup>1</sup>Department of Biomedical Engineering, Cornell University, Ithaca NY

### Abstract

Tumor draining lymph nodes are the first site of metastasis in most types of cancer. The extent of metastasis in the lymph nodes is often used in staging cancer progression. We previously showed that nanoscale TRAIL liposomes conjugated to human natural killer cells enhance their endogenous therapeutic potential in killing cancer cells cultured in engineered lymph node microenvironments. In this work, it is shown that liposomes decorated with apoptosis-inducing ligand TRAIL and an antibody against a mouse natural killer cell marker are carried to the tumor draining inguinal lymph nodes and prevent the lymphatic spread of a subcutaneous tumor in mice. It is shown that targeting natural killer cells with TRAIL liposomes enhances their retention time within the tumor draining lymph nodes to induce apoptosis in cancer cells. It is concluded that this approach can be used to kill cancer cells within the tumor draining lymph nodes to prevent the lymphatic spread of cancer.

### Keywords

Nanotechnology; liposomes; Tumor-draining lymph nodes; TRAIL; natural killer cells

### Introduction

It has been estimated that 29–37% of cancer patients with breast, colorectal and lung cancers are diagnosed with metastases in their tumor draining lymph nodes (TDLN) [1]. These patients are at a higher risk for distant organ metastases through the vast network of lymphatic capillaries. Lymph nodes (LN) are oval-shaped organs filled with immune cells where the lymphatic capillaries converge, providing an opportunity for the resident immune cells to act against virus infected host cells and cancer cells that may be present in the lymph fluid. An important subset of immune cells patrolling the LN is the natural killer (NK) cell population, representing about 1–5% of mononuclear cells [2]. Despite evidence of NK cell mediated anti-tumor immune response in the LN of experimental animals [3], the LN still remains the first site of metastasis in melanomas and carcinomas [4]. Tumor cell survival is promoted by primary tumor-induced NK cell abnormalities in the TDLN [5]. It has been

\*To whom correspondence should be addressed: mike.king@cornell.edu.

**Publisher's Disclaimer:** This is a PDF file of an unedited manuscript that has been accepted for publication. As a service to our customers we are providing this early version of the manuscript. The manuscript will undergo copyediting, typesetting, and review of the resulting proof before it is published in its final citable form. Please note that during the production process errors may be discovered which could affect the content, and all legal disclaimers that apply to the journal pertain.

shown that human NK cells in secondary lymphoid organs such as LN display a different phenotype [6], allowing distinction from the bulk of the NK cells present in the blood. This presents an opportunity to engineer endogenous NK cells in the TDLN to specifically kill cancer cells to prevent the lymphatic spread of cancer. NK cell mediated anti-tumor immune response often involves the expression of Tumor necrosis factor- $\alpha$  Related Apoptosis Inducing Ligand (TRAIL) on its surface, which initiates apoptosis by interacting with death receptors on cancer cells [7]. TRAIL has widely investigated as a potential therapeutic agent since its discovery in 1975 [8]. Despite the selectivity of TRAIL in inducing apoptosis in cancer cells, there are yet few promising reports on its clinical efficacy [9]. This has motivated several groups to design new formulations to address the limited clinical efficacy of TRAIL.

The advent of use of host immune cells to fight cancer has led to some innovative immunotherapeutic approaches. Several of these efforts have progressed to the clinic in the past decade, such as IL-2 therapy [10], ipilimumab [11] (anti-CTLA4 antibody) and chimeric antigen-receptor engineered T-cell therapy [12]. This has motivated the design of new immunotherapeutic approaches as an alternative to side-effect prone chemotherapy and radiation therapy often used in the treatment of advanced stages of cancer [13]. Nanotechnology-based immunotherapeutic approaches have received attention as a potential route of administering immunomodulatory cytokines/antibodies because of their ability to reduce systemic toxicity compared to conventional formulations [14]. The delivery of immunotherapeutic agents via nanoscale carriers has the advantages of (i) penetrating through the smallest capillaries dimensions, (ii) specifically targeting tumors when engineered with targeting moieties and (iii) eliciting a localized stimuli-sensitive response because of their capacity to release the immunotherapeutic drug in response to specific cues within the tumor such as pH, hypoxia etc. Nanoscale carriers such as liposomes have been FDA approved for use in chemotherapy and marketed as DOXIL (liposomal doxorubicin) [15] and Abraxane (albumin bound paclitaxel) [16]. Taking a cue from the body's natural defense mechanism, we previously showed that "super" natural killer cells formed through attachment of TRAIL-coated liposomes to NK cells via targeting antibody can effectively induce apoptosis in human cancer cell lines in engineered *in vitro* LN microenvironments [17]. When cocultured with human cancer cell lines that are known to metastasize to LN in experimental animal models, engineered super natural killer cells were able to induce apoptosis in cancer cells to a significantly higher degree compared to unmodified NK cells.

The goal of the present study was to determine if TRAIL liposomes targeted to NK cells that traffic to the tumor draining inguinal LN of mice bearing a subcutaneous human xenograft tumor could effectively prevent the metastasis of a primary tumor to the TDLN. Orthotopic models are also used for studying cancer metastasis in experimental animal models [18]. While orthotopic models have the advantage of providing a more realistic microenvironment for the primary tumor to metastasize, subcutaneous models are often used in studies investigating the lymphatic spread of cancer [19]. Here, we describe a therapeutic approach to target and kill cancer cells in the subcutaneous tumor draining inguinal LN by functionalizing natural killer cells with liposomes conjugated with the apoptosis-inducing ligand TRAIL, and an antibody against NK1.1 antigen expressed on murine NK cells (Fig.

1A). The functionalization of NK in the TDLN, creating “super” natural killer cells with sustained retention time in the TDLN, effectively prevents the lymphatic spread of the primary tumor.

## Materials and Methods

### Reagents and Antibodies

Bovine serum albumin (BSA), Paraformaldehyde (PFA), 4-(2-hydroxyethyl)-1-piperazineethanesulfonic acid (HEPES), NaCl, 2-Mercaptoethanol and chloroform (ACS grade) were all obtained from Sigma-Aldrich. Leibovitz’s L-15, Dulbecco’s Modified Eagle’s Medium (DMEM) and Hybri-care cell culture media were obtained from ATCC. RPMI 1640 cell culture media, penicillin-streptomycin (PenStrep), Fetal Bovine Serum (FBS), Ultra-low IgG FBS, Hank’s Based Salt Solution (HBSS), Phosphate Buffered Saline (PBS), NaHCO<sub>3</sub>, Non-Essential Amino Acids (NEAA), Traut’s reagent and DAPI stain were all purchased from LifeTechnologies. Recombinant soluble human tumor necrosis factor-related apoptosis-inducing ligand (sTRAIL), recombinant murine interleukin-2 (IL-2) and IL-15 were obtained from Peprotech. L- $\alpha$ -phosphatidylcholine from egg (Egg PC), ovine wool cholesterol (Chol), 1,2-distearoyl-*sn*-glycero-3-phosphoethanolamine-*N*-[methoxy (polyethylene glycol)-2000] (DSPE-mPEG2000) and 1,2-distearoyl-*sn*-glycero-3-phosphoethanolamine-*N*-[maleimide (polyethylene glycol)-2000] (DSPE-Mal-mPEG2000) were purchased from Avanti Polar Lipids. Mouse anti-human DR4 and DR5 conjugated to PE, Mouse anti-human TRAIL (primary Ab), FITC anti-mouse IgG (secondary Ab), mouse IgG1 isotype control, goat anti-mouse IgG and PE mouse IgG1 isotype control were all purchased from BioLegend. Anti-mouse CD3, CD11c, CD335 and B220 conjugated to APC along with isotype controls were purchased from eBioscience. Annexin-V FITC apoptosis detection kit was purchased from Trevigen. Liver activity detection kits for measuring serum levels of alanine aminotransferase (ALT) and aspartate aminotransferase (AST) were purchased from BioVision. Mouse NK cell isolation kit was purchased from Stemcell Technologies. Human TRAIL ELISA kit and mouse interferon- $\gamma$ (IFN- $\gamma$ ) ELISA kit were obtained from R&D systems and eBioscience, respectively. Protein G columns and buffers for isolating anti-NK1.1 antibody secreted by mouse hybridoma cell line were purchased from GE Healthcare Lifesciences. 7-Aminoactinomycin/carboxyfluorescein succinimidyl ester (7-AAD/CFSE) cell-mediated cytotoxicity assay kit were obtained from Cayman Chemicals. Luciferase used for *in vivo* bioluminescent imaging was purchased from Gold Biotechnology.

### Cell Lines and Cell Culture

The SW620 cell line established from cancer cells isolated from the tumor draining LN of a human patient with primary colon cancer (ATCC number CCL-227) was obtained from ATCC and cultured in L-15 medium supplemented with 10% (vol/vol) FBS and 100 U/mL PenStrep under humidified conditions at 37°C with 5% CO<sub>2</sub>. Murine melanoma cell line B16F0 (ATCC number CRL-6322) was obtained from ATCC and cultured in DMEM medium supplemented with 10% (vol/vol) FBS and 100 U/mL PenStrep under humidified conditions at 37°C with 5% CO<sub>2</sub>. Mouse hybridoma cell line PK136 (ATCC number HB191) secreting anti-NK1.1 antibody against murine NK cells was purchased from ATCC

and cultured in HybriCare medium supplemented with 10% ultralow IgG FBS and 1.5 g/L of NaHCO<sub>3</sub>. Hybridoma cell culture was maintained at a concentration between 1×10<sup>5</sup> and 1×10<sup>6</sup> cells/mL. For all experiments, cell viability was assessed by trypan blue exclusion dye before counting. Isolated mouse NK cells were cultured in RPMI media supplemented with 10% FBS (vol/vol), 1% NEAA, 50 μM 2-mercaptoethanol, 100 U/mL murine IL-2 and 10 U/mL murine IL-15.

### Mice and In Vivo Tumor Model

Cornell University's Institutional Animal Care and Use Committee (IACUC) approved all the experimental protocols and methods performed in mice. 6- to 8-week-old male C57BL/6 mice were purchased from Jackson Laboratory (Bar Harbor, ME, USA). Mice were housed at the Transgenic Mouse Core Facility at Cornell University in filter-top cages under pathogen-free conditions with free access to water and food. These mice were used for toxicology and pharmacokinetics experiments. 6- to 8-week-old male B6.129S7-*Rag1<sup>tm1Mom</sup>/J* mice (B6Rag1) were purchased from Jackson Laboratory. B6Rag1 mice have a “non-leaky” immunocompromised phenotype. They lack mature T-cells and B-cells allowing human cancer cell lines to propagate but have its innate immunity intact (high NK cell activity). The high NK cell activity is advantageous for evaluating the therapeutic efficacy of engineered liposomes directed towards NK cells in the tumor draining LN. The animals were weighed weekly and monitored for signs of distress by the Cornell Center for Animal Resources and Education (CARE) facility staff.

For spontaneous metastasis to the inguinal LN, luciferase-expressing SW620 cells (2×10<sup>6</sup> cells/100 μL of PBS) were injected subcutaneously into the lower left abdominal flank. After cancer cell injection, animals were monitored weekly for primary tumor growth and metastasis to the inguinal lymph node using an *in vivo* luciferase-based reporter assay. Luciferin was administered at 150 mg/kg per animal intraperitoneally using a 30G insulin syringe needle. Animals were placed under anesthesia using 2% isoflurane and imaged 10 min post-injection for maximum bioluminescence signal. Images were acquired at 10 s exposure time using a Xenogen IVIS 200 Imaging System. For quantification of total flux wherever reported, in-house developed region of interest (ROI) measurement tools were used to compare the signal intensity.

### Preparation of Liposomes

Multilamellar liposomes (10 mM in 1 mL) composed of EggPC, Chol, DSPE-mPEG2000 and DSPE-mPEG2000-maleimide at molar ratios 2:1:0.05:0.05 were prepared using a lipid extrusion method [20]. The maleimide functional group on DSPE-mPEG2000 allows for attachment of thiolated proteins. Briefly, lipids were allowed to form a thin film by mixing them in desired proportions and leaving them overnight in a vacuum glass chamber to ensure complete removal of chloroform. They were then hydrated in a buffer composed of 20 mM HEPES and 150 mM NaCl in PBS at pH 7.5. Hydrated lipids formed multilamellar vesicles which were then disrupted by 15 freeze (2 min)/thaw (3 min) cycles before extrusion. The lipid suspension was then forced through a polycarbonate filter with successively smaller pore size (400 nm, 200 nm and 100 nm) mounted on a holder in a heating block (Avanti<sup>®</sup> mini-extruder). The temperature was maintained at 60 °C, which is

above the phase transition temperature of the lipids. Anti-NK1.1, TRAIL and anti-mouse IgG were thiolated using 1 mM Traut's reagent following a protocol supplied by the manufacturer. Excess Traut's reagent was removed using a desalting column. The modification of TRAIL and Anti-NK1.1 via Traut's reagent does not alter their biological activity (data not shown). Thiolated proteins were conjugated to the liposome surface by incubating them with liposomes overnight at 4°C (500 nM of TRAIL and 500nM of anti-NK1.1). To remove unbound proteins, liposomes were diluted in liposome buffer and ultracentrifuged at  $100,000 \times g$  for 6 hr at 4°C. Freshly prepared nanoscale liposomes were characterized using a Zetasizer (Malvern Instruments Ltd.) to ensure successful conjugation of proteins. Unconjugated liposomes were measured to be  $94.87 \pm 2.8$  nm in diameter with a zeta potential of  $-4.8 \pm 3.2$  mV and conjugated liposomes were measured to be  $138 \pm 6.2$  nm in diameter with a zeta potential of  $-11.8 \pm 6.7$  mV. Liposome-bound TRAIL was quantified using ELISA following solubilization of liposomes in 0.5% Tween 20 buffer. The concentration of TRAIL was determined to be 26.5 ng/mL, which is equivalent to 3.6 ng/mg of lipid.

### TRAIL Sensitivity Experiment

SW620 cells were seeded in 6-well plates at a seeding density of 100,000 cells per mL and allowed to proliferate for one day before being treated with TRAIL. Media was changed before TRAIL treatment to ensure the removal of floating cells. Cells were then incubated with media containing 0–100 ng/mL of TRAIL and cultured for 24 hr. A standard colorimetric MTT assay was performed after 24 hr in culture to determine the percentage of viable cells. The absorbance was measured at 690 nm using a microplate reader (Bio-Tek Instruments). The absorbance was normalized with respect to untreated control and the viability reported as percentages.

### Mouse Natural Killer Cell Isolation

Mice were euthanized by CO<sub>2</sub> administration following an IACUC-approved protocol. The left and right inguinal LN were isolated from mice by making a small incision above the hind limb region near the abdomen. The isolated LN were digested by placing the LN in between frosted slides immersed in cell culture media. The resulting single cell suspension from the LN tissue was then used for downstream analysis such as flow cytometry wherever appropriate. NK cells from single cell suspensions obtained from the inguinal LN were isolated using an EasySep mouse NK cell enrichment kit following a protocol supplied by the manufacturer. The purity of the NK cell isolation was verified via flow cytometry by labeling the isolated cells with anti-CD335 to identify NK cells and CD3 to identify T-cells.

### Natural Killer Cell Activity Assays

NK cells isolated from the inguinal LN of mice that received different treatments were cultured *in vitro* to measure their activity. Growth rate, IFN- $\gamma$  secretion, and cytotoxicity were measured to examine differences in NK cell activity. Isolated NK cells were seeded in 48-well plates at a seeding density of  $10^3$  cells/well. The number of cells was counted on the 3<sup>rd</sup> and 7<sup>th</sup> day of culture using an automated cell counter (BioRad). The media conditioned by cultured NK cells was assayed for levels of IFN- $\gamma$  on the 1<sup>st</sup> and 7<sup>th</sup> day of culture using

ELISA. The cytolytic activity of NK cells was quantified using a 7-AAD/CFSE staining kit. It has been shown that murine NK cells can induce cytotoxicity in the cultured mouse melanoma cell line B16F0 [21]. To determine NK cell cytotoxicity, B16F0 melanoma cells (Target cells) were pre-labeled with a green fluorescent probe CFSE and cultured with murine NK cells (Effector) at predetermined target/effector cell ratios (5:1, 10:1 and 15:1). The cell mixture was incubated overnight to allow for NK cell cytolytic activity. The cell mixture was incubated with 7-AAD (fluorescent marker for dead cells) and analyzed using flow cytometry (Guava easyCyte™ flow cytometer, Millipore) to determine the degree of cytotoxicity of NK cells.

### Pharmacokinetic Experiments

To determine how long TRAIL/Anti-NK1.1 liposomes can remain bound to the surface of NK cells in the inguinal LN, wild-type C57BL/6 mice received subcutaneous injections of buffer, TRAIL/IgG or TRAIL/Anti-NK1.1 liposomes (0.8 mg lipids in 50µL) (three mice per group) on both the left and the right abdominal flanks. The left and right inguinal LN were harvested 24 hr post-injection and dissociated single cell suspensions from all of the LN were pooled together to isolate NK cells. The isolated NK cells were then deposited onto microscope slides using a Shandon Cytospin 3 (Harlow Scientific). The fixed and permeabilized cells were then stained with antibody against anti-human TRAIL (to label TRAIL on the liposomes) followed by a FITC conjugated secondary antibody and DAPI to label the nuclei. The cells were then imaged using a Zeiss 710 laser scanning confocal microscope and 10 confocal images for each time point were used to quantify the percentage of NK cells bound with liposomes. For the TRAIL/Anti-NK1.1 group, additional time points of t=48, 72 and 96 hr were investigated to quantify the percentage of NK cells bound with liposomes.

### Treatment Groups and Conditions

Based on the size of the primary tumor 2 weeks after subcutaneous tumor implantation, 25 mice were divided into 5 groups. Animals within each group received injections of buffer, soluble TRAIL (26.5 ng/mL), TRAIL/IgG liposomes, Anti-NK1.1 liposomes or TRAIL/Anti-NK1.1 liposomes. Each group received 50 µL subcutaneous injections (0.8 mg of lipids) directly adjacent to the primary tumor. The animals were treated on every third day based on observations from the pharmacokinetics of TRAIL/Anti-NK1.1 liposomes. By the end of week 6, mice in the control groups showed signs of distress and pain owing to ulceration and tissue necrosis of the skin overlying the developing tumor. This dictated the humane end point of the study. At the end of 6 weeks, mice in all the treatment groups were euthanized and inguinal LN harvested and used for further downstream experiments.

### Ex Vivo Bioluminescence Imaging and Histology

For assessing the tumor burden in the inguinal LN, harvested LN were placed in PBS containing 300µg/mL of D-luciferin. The organs were immersed for 5 min at 37°C before imaging. The LN were then arranged adjacent to each other in a black tape-covered cell culture lid and imaged at 1 s exposure time using a Xenogen IVIS 200. An in-house built ROI tool was used to quantify the signal intensity from individual LN to compare the extent of tumor burden in the inguinal LN between different treatment groups. The LN were then

transferred to 4% PFA overnight at room temperature. Representative LN from each treatment group were imaged using a digital camera and sent to the Histology Laboratory at Cornell University for H&E staining and scoring by a veterinary pathologist.

### Toxicology Experiments

Previous studies from our lab have shown that TRAIL liposomes do not induce cell death in human leukocytes, endothelial cells [22] and NK cells [17]. We used wild-type mice for toxicology experiments to evaluate the effect of TRAIL liposomes on T-cells, which are known to be sensitive to TRAIL [23]. On the contrary, there are studies that suggest that despite expressing receptor for TRAIL, T-cells and NK cells are resistant to TRAIL due to the expression of decoy receptors and cFLIP that inhibits the TRAIL pathway [24]. To determine the effect of TRAIL/Anti-NK1.1 on local lymph node tissue, non-tumor bearing wild-type C57BL/6 mice received TRAIL/Anti-NK1.1, TRAIL/IgG, or buffer injections subcutaneously (three mice per group) once every 3 days. After 6 weeks of treatment, inguinal LN were harvested and dissociated into single cell suspensions. The cells were analyzed using an Annexin-V FITC and Propidium Iodide (PI) apoptosis detection kit. The assay is based on the ability to differentiate cells in different stages of apoptosis. Annexin-V is a marker for cells undergoing apoptosis and PI is impermeable to live cells and apoptotic cells, but stains dead cells by binding tightly to the nucleic acid. The labeled cells from inguinal LN were analyzed using flow cytometry to quantify the proportion of viable cells. To assess liver toxicity owing to TRAIL administration, serum levels of alanine aminotransferase (ALT) and aspartate aminotransferase (AST) were measured at the end of the study using a colorimetric detection kit (BioVision). Serum was isolated from whole blood of animals in the different treatment groups at the conclusion of the experiment and the concentrations of ALT and AST were determined using a protocol provided by the manufacturer. Toxicity to liver was also assessed by H&E staining of the collected liver tissue.

### Flow Cytometry

The expression of death receptors in SW620 cells, expression of NK1.1 antigen on NK cells isolated from the inguinal LN of a wild-type C57BL/6 mouse, and the interaction of subcutaneously injected liposomes with different types of cells within the LN were analyzed on a Guava easyCyte™ flow cytometer using appropriate fluorescent antibodies and their corresponding isotype controls.

### Statistical Analysis

Where appropriate, pairwise differences in the bioluminescent tumor signals were analyzed at selected time points using the Wilcoxon rank-sum test. All statistical analyses were performed using GraphPad Prism 6.0 for Mac OS X (GraphPad software). Based on pilot *in vivo* experiments, total sample sizes of 5 mice per group achieved 80% power to detect a difference of at least 1.93 standardized units using the Dunnett multiple comparison test (3 comparisons against control) at the  $\alpha=0.05$  groupwise significance level. Significance analysis for NK cell activity assays, liver enzyme activity assays, Annexin-V/propidium iodide assay were analyzed using Student's t-test at the  $\alpha=0.05$  significance level.

## Results

### Pharmacokinetics of TRAIL/Anti-NK1.1 liposomes

To assess the relative distribution of TRAIL/Anti-NK1.1 liposomes within the inguinal LN, we injected liposomes subcutaneously on the lower left and right abdominal flanks. Subcutaneously injected TRAIL/Anti-NK1.1 liposomes remained bound to NK cells within the skin draining inguinal LN 24 hr post-injection with very minimal interaction with other cell types in the LN (Fig. 1B). To characterize liposome binding to different cell subpopulations within the LN, LN were isolated from mice that received subcutaneous injection of buffer, TRAIL/IgG liposomes, naked liposomes or TRAIL/Anti-NK1.1 liposomes 24 hr post injection. The isolated cells were labeled with B220, CD3, CD11c, CD335 and CD11b antibodies to label B-cells, T-cells, dendritic cells, NK cells and macrophages, respectively. The cells were also labeled with anti-TRAIL antibody to label human TRAIL on the surface of liposomes. Minimal adhesion of TRAIL/Anti-NK1.1 liposomes was observed for B-cells, T-cells and dendritic cells. However, CD335+ NK cells from mice that received TRAIL/Anti-NK1.1 liposome injections showed a significant shift in fluorescent peak intensity thus confirming the specific interaction of liposomes with NK cells in the inguinal LN (Fig. 1B). Additionally, NK cells were isolated (Fig. S1A) and verified for the expression of NK1.1 antigen on its surface (Fig. S1B) using the anti-NK1.1 antibody isolated from a hybridoma cell line. Confocal micrographs of isolated NK cells show a gradual reduction in the number of liposome bound NK cells after subcutaneous drug delivery (Fig. 1C). About ~28% of NK cells were bound with liposomes at  $t=72$  hr and ~2% of NK cells were bound with liposomes at  $t=96$  hr (Fig. 1D).

### Characterization of in vivo tumor model

When SW620 cells expressing luciferase were injected subcutaneously into the lower abdominal flank, tumor development was observed at the site of injection 1 week after injection. Luciferase allows monitoring of the growth of the primary tumor and the establishment of inguinal LN metastasis using noninvasive whole body bioluminescence imaging (BLI) [25]. The growth of the primary tumor and the establishment of lymph node metastasis in the skin draining inguinal LN were monitored weekly using a Xenogen IVIS imager (Fig. 2A). By week 6 mice started to develop ulceration in the skin overlying the subcutaneous primary tumor and were characterized with impaired movement dictating a humane endpoint for the study. Quantification of the total amount of photons (total flux) emitted by luciferase expressing primary tumor indicated an uninterrupted growth of the primary tumor up to 6 weeks post-implantation (Fig. 2B). The pigment associated signal loss in C57BL/6 mice [26] allows for visualization of the primary tumor and inguinal lymph node metastasis when the animals were imaged on their ventral and dorsal side, respectively. Sequential imaging of inguinal LN after subcutaneous injection of luciferase-tagged SW620 cells demonstrated initial metastasis formation 2–3 weeks post tumor inoculation that developed into macroscopic metastasis during 3–6 weeks post tumor inoculation (Fig. 2B). The SW620 cell line was established from the primary tumor draining mesenteric LN of a human colon cancer patient. It has been reported to be a TRAIL-resistant cell line when compared to its isoclonal SW480 cell line established from the primary colon tumor [27]. Despite this, we found SW620 to be sufficiently sensitive to TRAIL over a range that

includes the TRAIL concentration on liposomes used in this study (Fig. S2). SW620 cells expressed death receptors that initiate TRAIL-mediated apoptosis (Fig. S2A) and were sensitive to TRAIL in a concentration-dependent manner (Fig. S2B). SW620 cells treated with 100ng/mL of TRAIL showed characteristic morphological features of cells undergoing apoptosis (rounded and detached) when compared to untreated controls with live cells (spindle shaped and attached) (Fig. S2C).

### Tumor burden in inguinal lymph nodes

To test the ability of TRAIL/Anti-NK1.1 liposomes to prevent the metastasis of primary tumors to the LN, 25 mice were divided into 5 groups based on the size of the primary tumor 2 weeks after tumor implantation to achieve matched tumor size in each group. At the beginning of week 3, each group received buffer, soluble TRAIL, TRAIL/IgG liposomes (to account for non-specific interaction), Anti-NK1.1 liposomes (carrier without TRAIL) or TRAIL/Anti-NK1.1 liposomes subcutaneously for 4 weeks on every 3<sup>rd</sup> day. Two mice under distress were sacrificed at the end of week 5, one each from the buffer and soluble TRAIL treatment groups, as recommended by Cornell veterinary staff. The animals were monitored weekly using BLI for the growth of the primary tumor (Fig. S3) and the tumor burden in the tumor draining inguinal LN (Fig. 3). Whole animal BLI indicated increased tumor burden in the skin draining inguinal LN in control groups (buffer, soluble TRAIL, TRAIL/IgG liposomes and Anti-NK1.1 liposomes) (Fig. 3A). The TRAIL/Anti-NK1.1 treatment group showed a dramatic reduction in the ability of the primary tumor to metastasize to the inguinal LN (Fig. 3A). Time series analysis of total flux from the luciferase reporter showed a dramatic reduction in tumor burden in the inguinal LN for TRAIL/Anti-NK1.1 treated mice throughout the study, whereas the total flux in control groups demonstrated a steady increase with time (Fig. 3B). There was no significant difference in tumor burden by the end of week 2 before treatment (Fig. 3C). However, at the end of week 6, comparison of the total flux from animals in different treatment groups showed a significant decline in tumor burden for the TRAIL/Anti-NK1.1 treatment group (Fig. 3D).

### Ex vivo analysis of harvested lymph nodes

At the conclusion of the study, inguinal LN were removed and *ex vivo* BLI imaging was performed on harvested LN to assess the extent of tumor burden in animals from different treatment groups. Interestingly, strong BLI signal was detected in inguinal LN harvested from control groups but no BLI signal was detected in the TRAIL/Anti-NK1.1 treatment group (Fig. 4A). The size and appearance of the LN isolated from TRAIL/Anti-NK1.1 treated mice closely resembled the LN isolated from mice in the aged-matched control group with no tumor. Numerical quantification of total flux from *ex vivo* BLI imaging shows a significant reduction in signal intensity for LN harvested from the treatment group (Fig. 4B). Metastasis to the inguinal LN was characterized by significantly enlarged LN tissue (Fig. 4C). Hematoxylin and Eosin (H&E) staining was performed on harvested LN sections and interpreted by an independent animal pathologist. The pathology results were consistent with the observations from *ex vivo* BLI analysis (Fig. 4C). The examined H&E sections from the control groups were reported to contain LN either partially or fully encapsulated by neoplastic cells. In addition to the presence of cancer cells in the periphery of the tissue, the

interior of the tissue was found to be infiltrated with glands, clusters and sheets of neoplastic cells surrounded by fibrous tissue and few lymphoid cells (Fig. 4C). Inguinal LN were completely replaced by tumor with scarcely present lymphoid follicles throughout the tissue section. In comparison, LN from TRAIL/Anti-NK1.1 treatment group were not enlarged or infiltrated by cells from the primary tumor (Fig. 4C).

### Effect of liposome treatment on NK cell activity, LN tissue and liver

We next investigated the effect of treatment on NK cell activity and toxicity to the local LN tissue. The conjugation of TRAIL liposomes to NK cells does not alter their activity. Results showed that NK cells isolated from the inguinal LN of mice treated with TRAIL/Anti-NK1.1 liposomes for 6 weeks showed no significant difference in growth rate, cytotoxic potential and cytokine secretion levels when compared to NK cells isolated from control mice (Fig. 5A, B and C). NK cells were isolated from mice that received buffer, TRAIL/IgG and TRAIL/Anti-NK1.1 liposome injections subcutaneously for 6 weeks. The isolated cells were cultured *in vitro* for up to 7 days. Their growth rates were compared by counting the number of cells on day 3 and day 7 of culture. Results showed that TRAIL/Anti-NK1.1 liposomes did not alter the growth rate of NK cells (Fig. 5A). It has been shown that mouse NK cells can induce apoptosis in murine melanoma cell line B16F0 [21]. Coculturing isolated NK cells with B16F0 melanoma cells at increasing proportions of isolated NK cells indicated that liposome conjugation does not alter their cytotoxic ability (Fig. 5B). Previous works demonstrate that mouse NK cells cultured in IL-2 containing media secrete interferon- $\gamma$  (IFN- $\gamma$ ) and this has been used as a metric for evaluating NK cell activity [28,29]. NK cells isolated from the different treatment groups showed no significant difference in IFN- $\gamma$  secretion levels (Fig. 5C). TRAIL/Anti-NK1.1 liposomes did not induce significant toxicity to the local LN tissue (Fig. 5D, E and F), consistent with our previous *in vitro* studies [17,22]. The morphology of cells isolated from the LN of animals that received subcutaneous injections of buffer, TRAIL/IgG and TRAIL/Anti-NK1.1 liposomes for 6 weeks did not show any characteristic features of cells undergoing apoptosis (Fig. 5D). The isolated cells were then analyzed using an Annexin-V and propidium iodide (PI) binding assay for determining the extent of apoptotic cells in the LN. The cells were classified into four categories based on the degree of Annexin-V and PI staining: viable cells (negative for Annexin-V and PI), early apoptotic cells (positive for Annexin-V only), late apoptotic cells (positive for Annexin-V and PI), and necrotic cells (positive for PI only). Flow cytometry scatter plots (Fig. 5E) and the percentage of viable cells (Fig. 5F) show no significant difference in cell viability, indicating that the liposome treatment did not cause harm to the local LN cells.

Previous studies have shown that hepatocytes in the liver can exhibit sensitivity to TRAIL at extremely high doses [30]. To assess liver toxicity arising from liposomal TRAIL administration, serum levels of alanine aminotransferase (ALT) and aspartate aminotransferase (AST) were measured after 6 weeks of liposome injections. Liver transaminases are common biomarkers of liver injury [31]. The concentrations of these intracellular transaminases in the serum are normally low, and their presence is indicative of damage to the membranes of hepatocytes undergoing apoptosis. The serum levels of liver enzymes and H&E stained sections of liver were assessed for common signs of

hepatotoxicity induced by TRAIL. Mice that received TRAIL/Anti-NK1.1 liposome injections showed no signs of hepatotoxicity as evidence by the absence of significant elevation in the serum levels of liver enzymes (Fig. S4A) and absence of significant apoptosis in H&E stained liver sections (Fig. S4B) as compared to mice that received buffer or TRAIL/IgG liposome injections. Further, no notable fluctuation in body weight in animals from different treatment groups was observed, although tumor-bearing animals show reduced body weight when compared to non-tumor bearing control mice (Fig. S5).

## Discussion

The LN often acts as a bridgehead for the lymphatic spread of cancer. Cancer cells in the LN often form micrometastatic lesions and then disseminate through the extensive network of lymphatic capillaries to result in distant organ metastasis [32]. NK cells in the LN and circulation elicit their anti-tumor immune response by expressing TRAIL on their surface. Alternatively they can also secrete vesicles containing cytotoxic proteins such as perforins and granzymes, that mediate cancer cell death [33]. Both of these pathways are known to impair cancer metastasis in experimental animal models [34,35]. But NK cell mediated anti-tumor immune response is dampened in tumor-bearing immunocompromised hosts [36]. In this work, we were interested in enhancing the therapeutic efficacy of NK cells in the TDLN by coating them with TRAIL liposomes, to evoke a TRAIL-mediated response in cancer cells. This approach largely relies on the TRAIL pathway owing to prior studies that demonstrate the ability of TRAIL receptor-deficient cancer cells to successfully metastasize to the lymph nodes [37,38]. The ability to culture NK cells *in vitro* has led to several studies that have explored the use of NK cells in anti-tumor immunotherapy [39,40]. However, overarching problems with current NK cell mediated therapeutic approaches include: systemic toxicity, immune rejection, and inability to elicit long lasting immune response to prevent future relapse [41].

It has been shown that human cancer cells injected subcutaneously in the lower abdominal flank of mice spontaneously metastasize to the skin draining inguinal LN [42]. We characterized the spontaneous LN metastasis of human colon cancer cell line SW620 in partially immunocompromised B6.129S7-*Rag1<sup>tm1Mom</sup>/J* (B6Rag1) mice (Fig. 2). The presence of functional NK cells in B6Rag1 was crucial for testing the efficacy of liposomes directed towards functional NK cells. The IC<sub>50</sub> of TRAIL on SW620 cells is approximately 25 ng/ml *in vitro*. Although the concentration of TRAIL on liposomes is 26.5 ng/mL, the presentation of TRAIL in its natural membrane bound form could potentially increase their bioactivity as suggested by other studies [43,44]. Since it is difficult to target LN via the intravenous route, other routes for drug delivery, such as subcutaneous, intraperitoneal and intramuscular injections are often used to deliver liposomes to LN [45][46]. It has been reported that NK1.1 expressing NK cells actively patrol the inguinal LN in B6Rag1 mice [47]. The pharmacokinetics of TRAIL/Anti-NK1.1 liposomes (Fig. 1) is consistent with works that demonstrate a highly motile population of NK cells that patrol mouse LN [48,49]. When comparing the extent of tumor burden in the tumor draining inguinal LN, TRAIL/Anti-NK1.1 liposomes were able to significantly reduce the incidence of LN metastasis in all 5 mice in the treatment group (Fig. 3 and 4). To eliminate any potential bias, mice were randomly divided into 5 treatment groups based on the size of the primary

tumor by the end of week 2. There was no significant difference in the size of primary tumor (Fig. S3C) and inguinal lymph node metastasis (Fig. 3C) among different treatment groups. The ability of TRAIL/Anti-NK1.1 liposomes to bind to NK cells to form “super” NK cells played a significant role in reducing the ability of tumor cells to metastasize to the draining LN. The soluble form of TRAIL or liposome bound TRAIL without the NK cell targeting antibody showed no significant effect in reducing the tumor burden in the TDLN (Fig. 3 and 4). Also, given that the uninterrupted but slow growth of the primary tumor in the TRAIL/Anti-NK1.1 treatment group (Supplementary Fig. 3), it is clear that complete elimination of the primary tumor is not necessary to prevent metastasis to the LN. The slower growth of the primary tumor in the treatment group could be due to tumor infiltrating super NK cells working to slow their growth. We found that there was no significant difference in the percentage of primary tumor infiltrating NK cells across all treatment groups (Supplementary Fig. 6). Given the low amount (1–5%) of tumor infiltrating NK cells along with the unmitigated growth of the primary tumor in all groups, we conclude that subcutaneously injected liposomes reach the TDLN via skin draining lymphatics and bind to TDLN-resident NK cells to elicit TRAIL-mediated apoptosis. It has been shown that subcutaneous injection of drug adjacent to the primary tumor is efficient in animal models for delivering drugs to the LN [50]. However, other routes of administration such intra-LN injections have been shown to be more efficient in lymphatic drug delivery in human clinical trials [51].

In this study, we demonstrated the ability of TRAIL liposomes conjugated to NK cells within the TDLN to prevent the metastasis of a subcutaneous primary tumor using a human xenograft model. The majority of cancers metastasize through the lymphatic system and LN metastasis is a negative prognostic factor in many cancers [52]. By targeting TRAIL liposomes to NK cells, their therapeutic potential is enhanced by presenting TRAIL in its natural form, bound to the surface of NK cells. In this case there is no need to force other type of cells such as dendritic cells, T-cells and B-cells to present TRAIL, which are often used for lymph node-targeted nanoparticle delivery [14]. Given the successful elimination of tumor cells from the TDLN, future work could be directed towards exploring other potential routes for liposome administration in an orthotopic syngeneic animal model with an intact immune system and testing the efficacy in patient LN derived NK cells and tumor cells after surgical procedures. The proposed approach holds several advantages for LN targeted tumor therapy: high uptake in the TDLN, ability to present the therapeutic substance to cancer cells in its natural form, and low toxicity to local LN tissue.

## Supplementary Material

Refer to Web version on PubMed Central for supplementary material.

## References

1. Steeg PS. Tumor metastasis: mechanistic insights and clinical challenges. *Nat Med.* 2006; 12:895–904.10.1038/nm1469 [PubMed: 16892035]
2. Poli A, Michel T, Thérésine M, Andrès E, Hentges F, Zimmer J. CD56bright natural killer (NK) cells: An important NK cell subset. *Immunology.* 2009; 126:458–65.10.1111/j.1365-2567.2008.03027.x [PubMed: 19278419]

3. Chen S, Kawashima H, Lowe JB, Lanier LL, Fukuda M. Suppression of tumor formation in lymph nodes by L-selectin-mediated natural killer cell recruitment. *J Exp Med.* 2005; 202:1679–89.10.1084/jem.20051473 [PubMed: 16352740]
4. Sleeman JP. The lymph node as a bridgehead in the metastatic dissemination of tumors. *Recent Results Cancer Res.* 2000; 157:55–81.10.1007/978-3-642-57151-0\_6 [PubMed: 10857162]
5. Cochran AJ, Huang RR, Lee J, Itakura E, Leong SPL, Essner R. Tumour immunology - Tumour-induced immune modulation of sentinel lymph nodes. *Nat Rev Immunol.* 2006; 6:659–70.10.1038/Nri1919 [PubMed: 16932751]
6. Fehniger TA, Cooper MA, Nuovo GJ, Cella M, Facchetti F, Colonna M, et al. CD56bright natural killer cells are present in human lymph nodes and are activated by T cell-derived IL-2: a potential new link between adaptive and innate immunity. *Blood.* 2003; 101:3052–7.10.1182/blood-2002-09-2876 [PubMed: 12480696]
7. Zamai L, Ponti C, Mirandola P, Gobbi G, Papa S, Galeotti L, et al. NK cells and cancer. *J Immunol.* 2007; 178:4011–6. [PubMed: 17371953]
8. Lim B, Allen JE, Prabhu VV, Talekar MK, Finnberg NK, El-Deiry WS. Targeting TRAIL in the treatment of cancer: new developments. *Expert Opin Ther Targets.* 2015:1–15.10.1517/14728222.2015.1049838
9. Lemke J, von Karstedt S, Zinngrebe J, Walczak H. Getting TRAIL back on track for cancer therapy. *Cell Death Differ.* 2014; 21:1350–64.10.1038/cdd.2014.81 [PubMed: 24948009]
10. Schwartzentruber DJ, Lawson DH, Richards JM, Conry RM, Miller DM, Treisman J, et al. gp100 peptide vaccine and interleukin-2 in patients with advanced melanoma. 2011; 36410.1056/NEJMoa1012863
11. Hodi FS, O’Day SJ, McDermott DF, Weber RW, Sosman JA, Haanen JB, et al. Improved survival with ipilimumab in patients with metastatic melanoma. 2010; 36310.1056/NEJMoa1003466
12. Porter DL, Levine BL, Kalos M, Bagg A, June CH. Chimeric antigen receptor-modified T cells in chronic lymphoid leukemia. 2011; 36510.1056/NEJMoa1103849
13. Rosenberg SA, Yang JC, Restifo NP. Cancer immunotherapy: moving beyond current vaccines. *Nat Med.* 2004; 10:909–15.10.1038/nm1100 [PubMed: 15340416]
14. Chandrasekaran S, King MR. Microenvironment of Tumor-Draining Lymph Nodes: Opportunities for Liposome-Based Targeted Therapy. *Int J Mol Sci.* 2014; 15:20209–39.10.3390/ijms151120209 [PubMed: 25380524]
15. O’Shaughnessy JA. Pegylated liposomal doxorubicin in the treatment of breast cancer. *Clin Breast Cancer.* 2003; 4:318–28.10.3816/CBC.2003.n.037 [PubMed: 14715106]
16. Baba K. Pharmaceutical properties of Abraxane and highlight of its clinical study. *Drug Deliv Syst.* 2013; 28:180–8.10.2745/dd.28.180
17. Chandrasekaran S, McGuire MJ, King MR. Sweeping lymph node micrometastases off their feet: an engineered model to evaluate natural killer cell mediated therapeutic intervention of circulating tumor cells that disseminate to the lymph nodes. *Lab Chip.* 201410.1039/C3LC50584G
18. Wang X, An Z, Geller J, Hoffman RM. High-malignancy orthotopic nude mouse model of human prostate cancer LNCaP. *Prostate.* 1999; 39:182–6. [PubMed: 10334107]
19. Thelen A, Scholz A, Benckert C, Von Marschall Z, Schröder M, Wiedenmann B, et al. VEGF-D promotes tumor growth and lymphatic spread in a mouse model of hepatocellular carcinoma. *Int J Cancer.* 2008; 122:2471–81.10.1002/ijc.23439 [PubMed: 18338756]
20. Szoka F, Papahadjopoulos D. Comparative Properties and Methods of Preparation of Lipid Vesicles (Liposomes). *Annu Rev Biophys Bioeng.* 1980; 9:467–508.10.1146/annurev.bb.09.060180.002343 [PubMed: 6994593]
21. Lakshmikanth T, Burke S, Ali TH, Kimpfler S, Ursini F, Ruggeri L, et al. NCRs and DNAM-1 mediate NK cell recognition and lysis of human and mouse melanoma cell lines in vitro and in vivo. *J Clin Invest.* 2009; 119:1251–63.10.1172/JCI36022 [PubMed: 19349689]
22. Mitchell MJ, Wayne E, Rana K, Schaffer CB, King MR. TRAIL-coated leukocytes that kill cancer cells in the circulation. *Proc Natl Acad Sci U S A.* 2014; 2013:1–6.10.1073/pnas.1316312111
23. Schuster IS, Wikstrom ME, Brizard G, Coudert JD, Estcourt MJ, Manzur M, et al. TRAIL+ NK Cells Control CD4+ T Cell Responses during Chronic Viral Infection to Limit Autoimmunity. *Immunity.* 2015; 41:646–56.10.1016/j.immuni.2014.09.013 [PubMed: 25367576]

24. Mirandola P, Ponti C, Gobbi G, Sponzilli I, Vaccarezza M, Cocco L, et al. Activated human NK and CD8+ T cells express both TNF-related apoptosis-inducing ligand (TRAIL) and TRAIL receptors but are resistant to TRAIL-mediated cytotoxicity. *Blood*. 2004; 104:2418–24.10.1182/blood-2004-04-1294 [PubMed: 15205263]
25. Close DM, Xu T, Sayler GS, Ripp S. In vivo bioluminescent imaging (BLI): Noninvasive visualization and interrogation of biological processes in living animals. *Sensors*. 2011; 11:180–206.10.3390/s110100180 [PubMed: 22346573]
26. Rabinovich BA, Ye Y, Etto T, Chen JQ, Levitsky HI, Overwijk WW, et al. Visualizing fewer than 10 mouse T cells with an enhanced firefly luciferase in immunocompetent mouse models of cancer. *Proc Natl Acad Sci U S A*. 2008; 105:14342–6.10.1073/pnas.0804105105 [PubMed: 18794521]
27. Ndozangue-Tourguine O, Sebbagh M, Merino D, Micheau O, Bertoglio J, Breard J. A mitochondrial block and expression of XIAP lead to resistance to TRAIL-induced apoptosis during progression to metastasis of a colon carcinoma. *Oncogene*. 2008; 27:6012–22. [PubMed: 18560353]
28. Weigent DA, Stanton GJ, Johnson HM. Interleukin 2 enhances natural killer cell activity through induction of gamma interferon. *Infect Immun*. 1983; 41:992–7. [PubMed: 6411624]
29. Toomey JA. Cytokine requirements for the growth and development of mouse NK cells in vitro. *J Leukoc Biol*. 2003; 74:233–42.10.1189/jlb.0303097 [PubMed: 12885940]
30. Zheng SJ, Wang P, Tsabary G, Chen YH. Critical roles of TRAIL in hepatic cell death and hepatic inflammation. *J Clin Invest*. 2004; 113:58–64.10.1172/JCI200419255 [PubMed: 14702109]
31. Giboney PT. Mildly elevated liver transaminase levels in the asymptomatic patient. *Am Fam Physician*. 2005; 71:1105–10. [PubMed: 15791889]
32. Imoto S, Ochiai A, Okumura C, Wada N, Hasebe T. Impact of isolated tumor cells in sentinel lymph nodes detected by immunohistochemical staining. *Eur J Surg Oncol*. 2006; 32:1175–9.10.1016/j.ejso.2006.08.006 [PubMed: 16979316]
33. Trapani JA, Smyth MJ. Functional significance of the perforin/granzyme cell death pathway. *Nat Rev Immunol*. 2002; 2:735–47.10.1038/nri911 [PubMed: 12360212]
34. Smyth MJ, Cretney E, Takeda K, Wiltrot RH, Sedger LM, Kayagaki N, et al. Tumor necrosis factor-related apoptosis-inducing ligand (TRAIL) contributes to interferon gamma-dependent natural killer cell protection from tumor metastasis. *J Exp Med*. 2001; 193:661–70. [PubMed: 11257133]
35. Takeda K, Hayakawa Y, Smyth MJ, Kayagaki N, Yamaguchi N, Kakuta S, et al. Involvement of tumor necrosis factor-related apoptosis-inducing ligand in surveillance of tumor metastasis by liver natural killer cells. *Nat Med*. 2001; 7:94–100.10.1038/83416 [PubMed: 11135622]
36. Levy EM, Roberti MP, Mordoh J. Natural killer cells in human cancer: from biological functions to clinical applications. *J Biomed Biotechnol*. 2011; 2011:676198.10.1155/2011/676198 [PubMed: 21541191]
37. Grosse-Wilde A, Kemp CJ. Metastasis suppressor function of tumor necrosis factor-related apoptosis-inducing ligand-R in mice: Implications for TRAIL-based therapy in humans? *Cancer Res*. 2008; 68:6035–7.10.1158/0008-5472.CAN-08-0078 [PubMed: 18676822]
38. Grosse-Wilde A, Voloshanenko O, Lawrence Bailey S, Longton GM, Schaefer U, Csernok AI, et al. TRAIL-R deficiency in mice enhances lymph node metastasis without affecting primary tumor development. *J Clin Invest*. 2008; 118:100–10.10.1172/JCI33061 [PubMed: 18079967]
39. Childs RW, Berg M. Bringing natural killer cells to the clinic: ex vivo manipulation. *ASH Educ Progr B*. 2013; 2013:234–46.10.1182/asheducation-2013.1.234
40. Wu J, Lanier LL. Natural Killer Cells and Cancer. *Adv Cancer Res*. 2003; 90:127–56.10.1016/S0065-230X(03)90004-2 [PubMed: 14710949]
41. Salagianni M, Baxevanis CN, Papamichail M, Perez SA. New insights into the role of NK cells in cancer immunotherapy. *Oncoimmunology*. 2012; 1:205–7.10.4161/onci.1.2.18398 [PubMed: 22720243]
42. Yokoyama H, Nakanishi H, Kodera Y, Ikehara Y, Ohashi N, Ito Y, et al. Biological significance of isolated tumor cells and micrometastasis in lymph nodes evaluated using a green fluorescent

- protein-tagged human gastric cancer cell line. *Clin Cancer Res.* 2006; 12:361–8.10.1158/1078-0432.CCR-05-1963 [PubMed: 16428473]
43. Martínez-Lorenzo MJ, Anel A, Gamen S, Monlen I, Lasierra P, Larrad L, et al. Activated human T cells release bioactive Fas ligand and APO2 ligand in microvesicles. *J Immunol.* 1999; 163:1274–81. [ji\\_v163n3p1274](#) [pii]. [PubMed: 10415024]
44. De Miguel D, Basáñez G, Sánchez D, Malo PG, Marzo I, Larrad L, et al. Liposomes Decorated with Apo2L/TRAIL Overcome Chemoresistance of Human Hematologic Tumor Cells. *Mol Pharm.* 2013; 10:893–904.10.1021/mp300258c [PubMed: 23331277]
45. Xie Y, Bagby TR, Cohen MS, Forrest ML. Drug delivery to the lymphatic system: importance in future cancer diagnosis and therapies. *Expert Opin Drug Deliv.* 2009; 6:785–92.10.1517/17425240903085128 [PubMed: 19563270]
46. Oussoren C, Storm G. Liposomes to target the lymphatics by subcutaneous administration. *Adv Drug Deliv Rev.* 2001; 50:143–56.10.1016/S0169-409X(01)00154-5 [PubMed: 11489337]
47. Garrod KR, Wei SH, Parker I, Cahalan MD. Natural killer cells actively patrol peripheral lymph nodes forming stable conjugates to eliminate MHC-mismatched targets. *Proc Natl Acad Sci U S A.* 2007; 104:12081–6.10.1073/pnas.0702867104 [PubMed: 17609379]
48. Bajénoff M, Bajénoff M, Breart B, Breart B, Huang AYC, Huang AYC, et al. Natural killer cell behavior in lymph nodes revealed by static and real-time imaging. *J Exp Med.* 2006; 203:619–31.10.1084/jem.20051474 [PubMed: 16505138]
49. Beuneu H, Deguine J, Breart B, Mandelboim O, Di Santo JP, Bousso P. Dynamic behavior of NK cells during activation in lymph nodes. *Blood.* 2009; 114:3227–34. [PubMed: 19667398]
50. Harivardhan Reddy L, Sharma RK, Chuttani K, Mishra AK, Murthy RSR. Influence of administration route on tumor uptake and biodistribution of etoposide loaded solid lipid nanoparticles in Dalton's lymphoma tumor bearing mice. *J Control Release.* 2005; 105:185–98.10.1016/j.jconrel.2005.02.028 [PubMed: 15921775]
51. Senti G, Prinz Vavricka BM, Erdmann I, Diaz MI, Markus R, McCormack SJ, et al. Intralymphatic allergen administration renders specific immunotherapy faster and safer: a randomized controlled trial. *Proc Natl Acad Sci U S A.* 2008; 105:17908–12.10.1073/pnas.0803725105 [PubMed: 19001265]
52. Sleeman JP, Thiele W. Tumor metastasis and the lymphatic vasculature. *Int J Cancer.* 2009; 125:2747–56.10.1002/ijc.24702 [PubMed: 19569051]



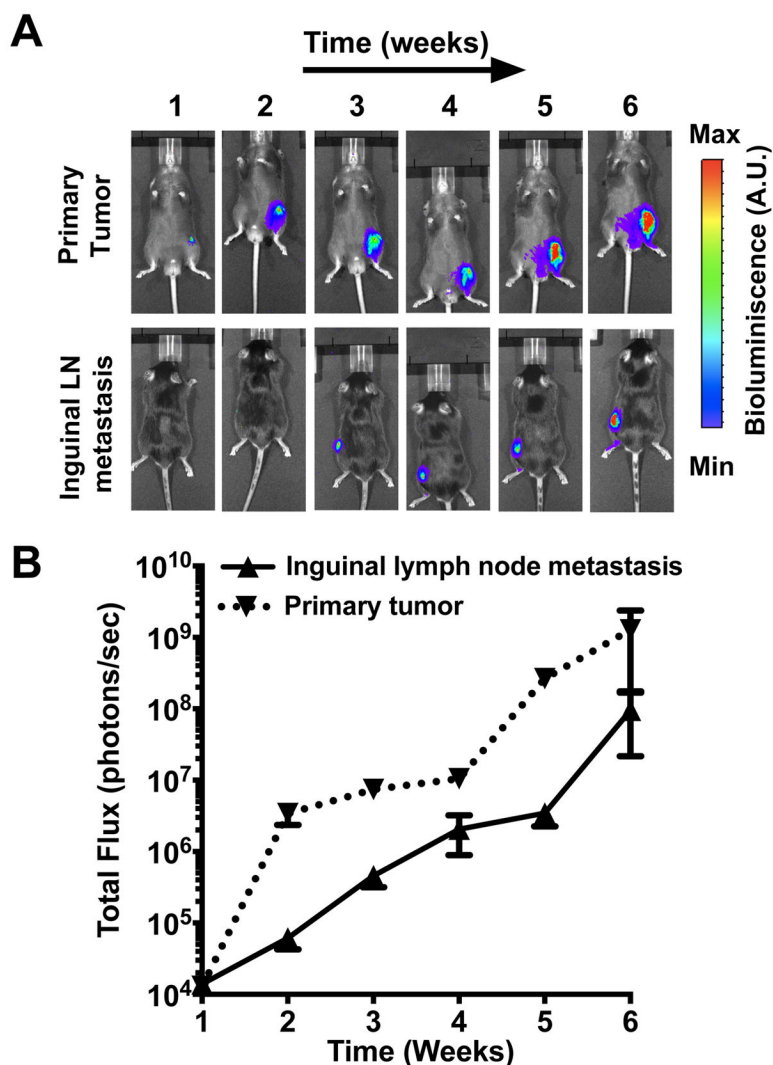


**Fig. 2. Characterization of *in vivo* tumor model**

(A) Sequential noninvasive bioluminescence imaging of B6Rag1 mice implanted with  $2 \times 10^6$  SW620-luc cells subcutaneously on the lower left abdominal flank shows the growth of a primary tumor and the development of metastasis in the tumor draining inguinal lymph node with time. Tumor development was monitored by luciferase signal, measured by *in vivo* imaging at week 1, 2, 3, 4, 5, and 6 after tumor implantation. The color scale indicates bioluminescence signal intensity. The pigment-associated signal loss allows the visualization of the primary tumor and inguinal lymph node metastasis separately when the animal is imaged on its back and front, respectively. (B) Quantification of total flux from a circular region of interest (ROI) around the primary tumor and inguinal lymph node metastasis. Each point represents the mean  $\pm$  standard deviation of total flux from 5 different mice. The photon flux increases with time, showing the growth of primary tumor and inguinal lymph node metastasis upon tumor implantation.

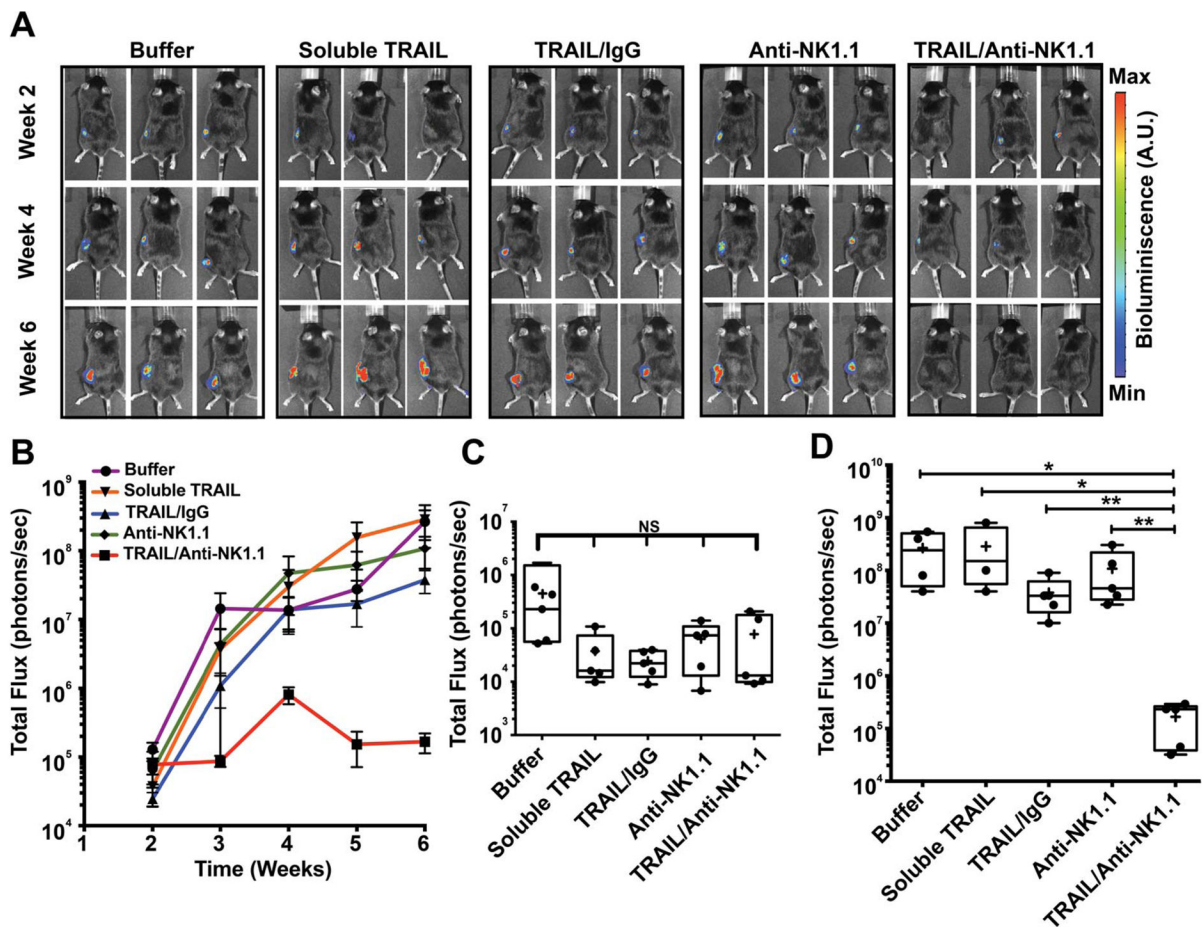


**Fig.3. Metastatic burden in the tumor draining inguinal lymph nodes**

(A) Sequential non-invasive bioluminescence imaging shows the growth of inguinal lymph node metastases in mice under different treatment conditions. Three representative mice per group are shown at week 2, 4 and 6 for each treatment condition. The color scale indicates bioluminescence signal intensity. (B) Quantification of total flux, indicating the tumor burden in the inguinal lymph nodes with time. Each point represents the mean  $\pm$  standard deviation for 5 mice at each time point (4 mice at week 6 for buffer and soluble TRAIL treatment groups). (C) Box and whisker plot comparing total flux from the inguinal lymph nodes in mice from different treatment groups at week 2. NS, Not Significant (Wilcoxon rank-sum test) (D) Box and whisker plot comparing the total flux from the inguinal lymph nodes in mice from different treatment groups at week 6. \* $p < 0.05$ , \*\* $p < 0.01$  (Wilcoxon rank-sum test) and  $n = 5$  mice per group (4 mice for buffer and soluble TRAIL treatment groups).

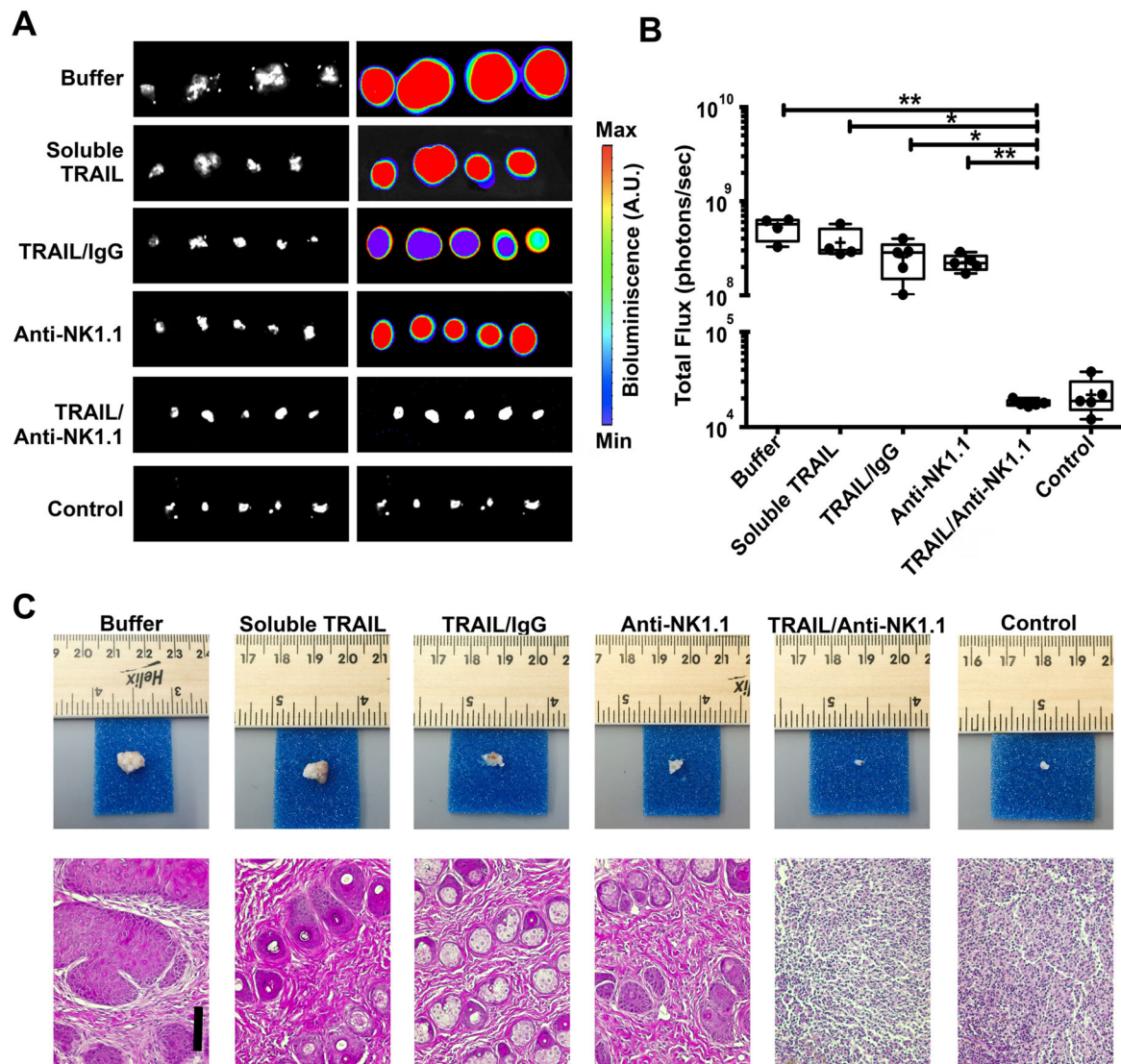


**Fig.4. Ex vivo analysis of harvested lymph nodes**

(A) Bright field and bioluminescence images of lymph nodes harvested from different control groups and treatment group at the end of the study. The color scale indicates bioluminescence signal intensity. (B) Quantification of total flux from harvested lymph nodes in each treatment group. \* $p < 0.05$ , \*\* $p < 0.01$  (Wilcoxon rank-sum test) and  $n = 5$  mice per group (4 mice for buffer and soluble TRAIL treatment groups). (C) Images (Color and H&E stained sections) of inguinal lymph nodes harvested from a representative mouse in each treatment group. Scale bar =  $200\mu\text{m}$ .

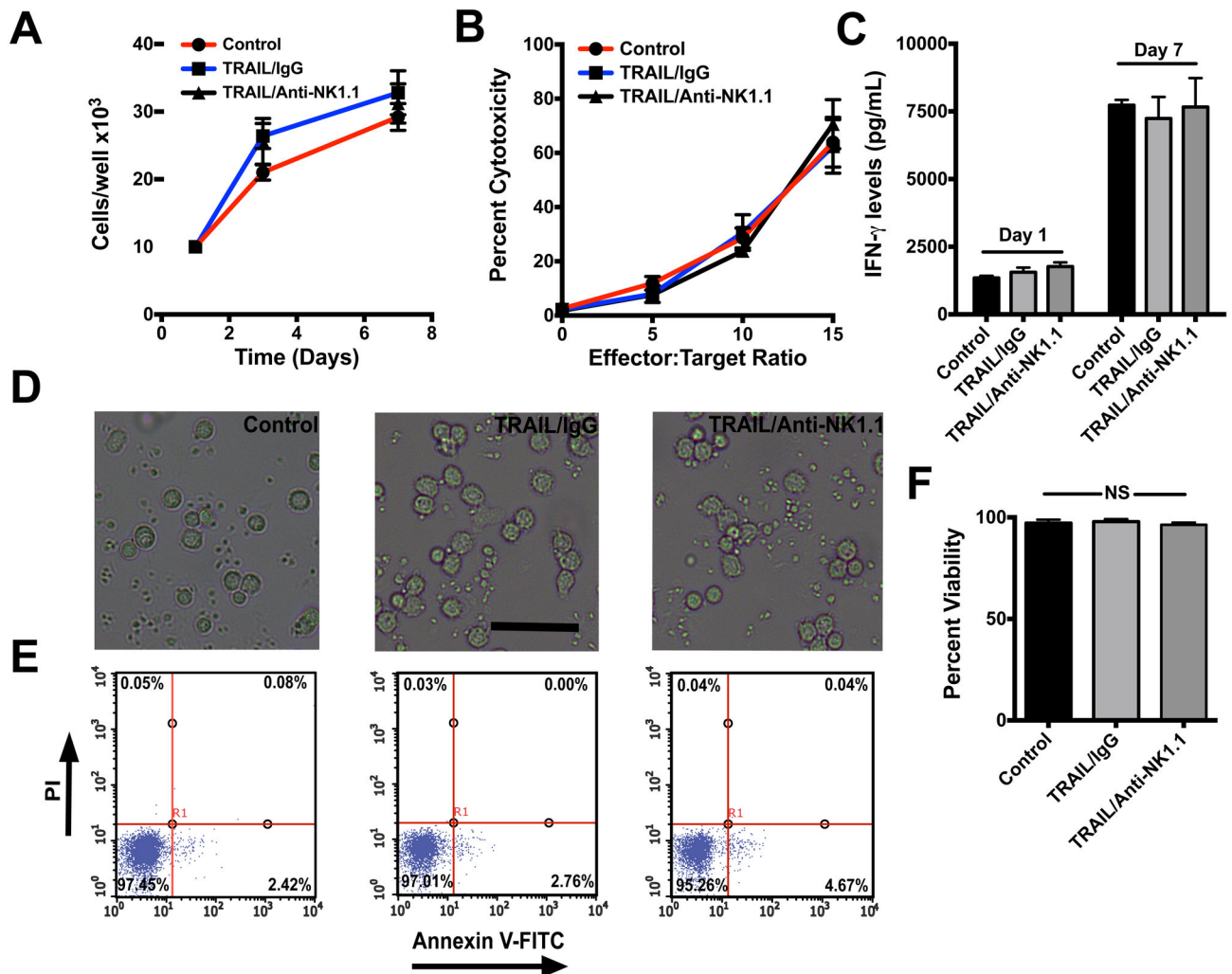


**Fig. 5. Mouse NK cell activity assays and toxicity to LN tissue**

(A) Growth of NK cells isolated from the untreated and treated groups shows no significant difference in their growth based on cell counts on day 3 and day 7 of culture.  $n=3$  for all samples. Each point represents the mean  $\pm$  standard deviation of the number of cells. (B) Triplicate cultures containing different proportions of effector (NK cells from control and treatment groups) to target cells (B16F0 murine melanoma cells) were initiated one day after isolating NK cells.  $n=3$  for all samples. Each point represents the mean  $\pm$  standard deviation of the percentage cytotoxicity of NK cells isolated from each treatment group. (C) The media conditioned by isolated NK cells was assayed for IFN- $\gamma$  levels on day 1 and day 7 of culture using an ELISA kit.  $n=3$  for all samples. Bars represent mean and standard deviation of IFN- $\gamma$  levels from each treatment condition. (D) Representative images of cells isolated from the inguinal lymph nodes of control and TRAIL/IgG and TRAIL/Anti-NK1.1 treated C57BL/6 mice 6 weeks after treatment. Scale bar=100  $\mu$ m. (E) Representative Annexin-V/propidium iodide (PI) flow cytometry scatter plots of cells isolated from untreated mice and those treated with TRAIL/IgG liposomes and TRAIL/Anti-NK1.1 liposomes. (F) Percent

viability of lymph node cells after various treatments. n=3 for all samples. Bars represent the mean  $\pm$  standard deviation for each treatment group. NS, not significant (Student t-test).

Author Manuscript

Author Manuscript

Author Manuscript

Author Manuscript